Self-consistent *GW* determination of the interaction strength: Application to the iron arsenide superconductors

A. Kutepov,[1] K. Haule,[1] S. Y. Savrasov,[2] and G. Kotliar[1]
[1]*Department of Physics, Rutgers University, Piscataway, New Jersey 08854, USA*
[2]*Department of Physics, University of California, Davis, California 95616, USA*
(Received 6 May 2010; revised manuscript received 21 June 2010; published 9 July 2010)

We introduce a first principles approach to determine the strength of the electronic correlations based on the fully self-consistent *GW* approximation. The approach provides a seamless interface with dynamical mean field theory, and gives good results for well studied correlated materials such as NiO. Applied to the recently discovered iron arsenide materials, it accounts for the noticeable correlation features observed in optics and photoemission while explaining the absence of visible satellites in x-ray absorption experiments and other high energy spectroscopies.

DOI: 10.1103/PhysRevB.82.045105 PACS number(s): 71.27.+a, 71.30.+h

I. INTRODUCTION

Many metals, semiconductors, and insulators are well described by the "standard model" of solid state physics. In this picture the excitations are band electrons, and their dispersion can be computed quantitatively in perturbation theory starting from the density functional theory using the *GW* method.[1] When this standard model fails, we talk about strongly correlated electron systems. The presence of strong correlations is debated with each new material discovery, as for example in the context of the iron pnictide superconductors. On the experimental side, controversies arose because optical experiments revealed significant mass renormalizations[2–4] while x-ray absorption, core level spectroscopies and resonant inelastic x-ray scattering indicated the absence of satellite peaks,[5,6] which are standard fingerprints of strong correlations. Photoemission studies indicate that the overall bandwidth is narrowed by a factor of two[7,8] but substantially larger mass renormalizations are present near the Fermi level.[9] Similar controversies arose within the first principles approaches to the treatment of correlations with some theoretical studies supporting the notion of weak correlations,[10–14] while others advocate a more correlated picture.[15–18] To make progress on this issues one needs to develop fully *ab initio* tools for addressing the problem of determining the strength of correlations and test their predictions against experiments.

In this paper, we present a first principles methodology for evaluating the strength of the correlations based on the self-consistent *GW* method. This approach has been shown to predict accurate total energy,[19,20] and we expect to obtain reliable estimates for the interaction strength since this quantity can be thought as a second derivative of the total energy with respect to the occupation of the correlated orbitals. We test successfully the method on the well-studied example of a correlated material NiO, and then we apply it to a prototypical iron pnictide $BaFe_2As_2$. We find that the correlations in iron pnictides are strong, as pointed out in Refs. 15–18 but unlike earlier studies our *ab initio* method accounts for the absence of well defined Hubbard bands in the spectral functions. Our results are thus in excellent agreement with experiment and reconcile the results of apparently conflicting spectroscopies.

II. METHOD

We start with the one-particle electron Green's function in the solid, G, which is measurable in photoemission experiments. We split it into $G^{-1}=G^{0^{-1}}+\Sigma$, where G^0 describes the noninteracting system of electrons, and Σ is the frequency dependent self-energy. Both G and Σ are matrices in $\mathbf{r},\mathbf{r}'$. The electrons interact among themselves via the Coulomb interaction $V_c(\mathbf{r},\mathbf{r}')=\frac{1}{|\mathbf{r}-\mathbf{r}'|}$, however, the mobile electrons screen it and is therefore useful to reformulate the problem in terms of a screened Coulomb interaction W defined by $W=V_c/(1+V_c\Pi)$ (Refs. 1 and 21) where Π is the exact polarization function.

Dynamical mean field theory (DMFT) maps the many body problem in the solid to that of a correlated *atomic* shell embedded in an effective medium. The medium is described by an energy dependent Weiss field $\mathcal{G}^0$, which obeys the following equation

$$\mathcal{G}^{0^{-1}} = G^{-1}_{local} + \Sigma_{local}. \tag{1}$$

Here, G_{local} and Σ_{local} are the local Green's function and the local self-energy, respectively.

The electrons in the renormalized atom feel an effective retarded Coulomb interaction $U(\omega)$. Just like the Weiss field $\mathcal{G}^0$ of the atom reflects the delocalizing effect of the medium at the single particle level, the Weiss field $U(\omega)$ captures the screening of the interaction due to the presence of the other atoms. The Weiss field at the two particle level $U(\omega)$ obeys the following relation

$$U^{-1} = W^{-1}_{local} + \Pi_{local}, \tag{2}$$

where Π_{local} and W_{local} are the local polarization function and the local screened interaction, respectively. The bare local propagators $\mathcal{G}^0(\omega)$ and bare interaction $U(\omega)$ are chosen so as to give the exact G_{local} and W_{local} when all the local Feynman diagrams are summed up. Equations (1) and (2) are a version of the extended-DMFT equations studied for simplified models in Refs. 22 and 23. The key idea of this work is to use this approach to estimate the correlation strength in the solid, and illustrate the power of the method by a practical realistic self-consistent implementation.

The approach shares ideas with other methods to compute the local interaction matrix U. Like constrained local density approximation (LDA), it defines correlations on a correlated *orbital*. It adopts the philosophy of the constrained random phase approximation (RPA) method,[24,25] which divides the *bands* into a set that belongs to the low-energy model, and the rest of the bands, which contribute to screening. However, instead of the bands, our method uses orbitals to divide the polarization operator of the lattice into a local part, involving the correlated orbital, and the rest, which screens the local interaction.

We now describe the steps required for the practical implementation of the method and its interface with LDA+DMFT (Ref. 26): (i) We perform a *fully self consistent GW* calculation.[1] (ii) We evaluate G_{loc} and W_{loc} using the projector $P(\mathbf{r}\mathbf{r}',tL_1L_2)$, defined in Ref. 27: $G^t_{local\ L_1L_2}=\int d\mathbf{r}P(\mathbf{r}\mathbf{r}',tL_1L_2)G(\mathbf{r}\mathbf{r}')$ and $W^t_{local\ L_4L_1;L_3L_2}=\int P(\mathbf{r},tL_4L_1)W(\mathbf{r}\mathbf{r}')P(\mathbf{r}'\mathbf{r}',tL_3L_2)d\mathbf{r}d\mathbf{r}'$. t is the atom index and $L=(l,m)$ is the angular momentum index. (iii) We evaluate $\Sigma_{loc}(\tau)=W_{local}(\tau)G_{local}(-\tau)$ and $\Pi_{loc}(\tau)=G_{local}(\tau)G_{local}(-\tau)$. We use Eq. (2) to evaluate $U(\omega)$, which we now denote by U^{GW}. (iv) We also evaluate the hybridization function $\Delta_{GW}(\omega)$ using Eq. (1) and identity $\mathcal{G}^{0^{-1}}_{GW}=\omega-E_{imp}-\Delta_{GW}$. Δ_{GW} contains the coupling of the correlated orbitals to the valence states of the system $\Delta_L(\omega)$, and to the semicore states $\Delta_H(\omega)$, and can thus be represented as $\Delta(i\omega)=\int d\varepsilon[\Delta_L(\varepsilon)+\Delta_H(\varepsilon)]/(i\omega-\varepsilon)$. In LDA+DMFT the hybridization to these semicore state is eliminated resulting in Δ_L, which is connected to GW hybridization by $\Delta_{GW}(i\omega)=\Delta_L(i\omega)-i\omega\alpha$, where $\alpha\approx\int d\varepsilon\Delta_H(\varepsilon)/\varepsilon^2$. This factor is then absorbed by rescaling of the field $\psi\rightarrow\psi/\sqrt{1+\alpha}$ and consequently the interaction matrix used in the LDA+DMFT calculation becomes $U_{LDA+DMFT}=U^{GW}(\omega=0)/(1+\alpha)^2$. This renormalization is usually very small, and in $BaFe_2As_2$ is $\alpha\approx0.05$.

We use this fully *ab initio* method to determine the interaction matrix strength U^{GW} and the occupancy of the d orbital n_d, which fixes the double-counting correction of LDA+DMFT. With this input, the LDA+DMFT method becomes a fully *ab initio* method.

The effective interaction obtained with this method is a general symmetric tensor with four indices $\Sigma_{\{m_i\},\sigma\sigma'}U_{m_4,m_3,m_2,m_1}\psi^\dagger_{m_4\sigma}\psi^\dagger_{m_3\sigma'}\psi_{m_2\sigma'}\psi_{m_1\sigma}$. It is useful to inquire to which extent this interaction can be approximated in terms of Slater integrals $F^{\{l\}}_k$, where k runs over $0,\ldots2l$. The optimal determination of this parameters is done with the projector

$$F^{\{l\}}_k=\sum_{m_1,m_2,m_3,m_4}\frac{1}{\mathcal{N}_{l,k}}\frac{4\pi}{2k+1}\langle Y_{lm_4}|Y_{km_4-m_1}|Y_{lm_1}\rangle \times U^{GW}_{m_4m_3m_2m_1}\langle Y_{lm_3}|Y^*_{km_2-m_3}|Y_{lm_2}\rangle. \quad (3)$$

Here $\mathcal{N}_{l,0}=(2l+1)^2$, $\mathcal{N}_{l=2,k=1}=5(2/7)^2$ and $\mathcal{N}_{l=2,k=2}=(10/21)^2$. The quality of the projection is excellent and can be seen by recomputing the Coulomb repulsion from the Slater integrals and comparing the resulting U^{atom} with the full U matrix. We mention in passing that the naive Hartree-Fock like estimation of Slater integrals $J=\langle U_{mm'mm'}\rangle_{m\neq m'}$, $F_2=14/1.625J$, and $F_4=8.75/1.625J$, can lead to a substantial underestimation of Slater integrals.

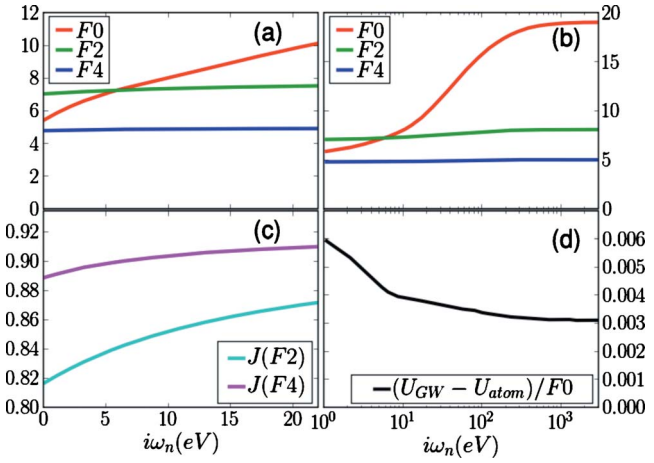

FIG. 1. (Color online) (a) and (b) Slater integrals versus Matsubara frequency as computed by fully self-consistent GW method, (c) corresponding Hund's coupling strength J, and (d) the difference between the GW Coulomb interaction and its Slater parameterization.

III. RESULTS

We first test our method in an arc-typical charge transfer insulator NiO. We get the following static values of the Slater integrals $F_0=7.9$ eV, $F_2=10$ eV, and $F_4=6.7$ eV. If the Hund's parameter J is computed from $F_2(F_4)$ we get $J(F_2)=1.16$ eV($J(F_4)=1.24$ eV). When these parameter are used in LDA+DMFT, the agreement between the theory and experiment is very good.[28] We mention in passing that when the GW screened interaction and polarization are computed from the LDA Kohn-Sham states (non-self-consistent GW) we get slightly smaller interaction strength $F_0\approx7.2$ eV.

Next we turn to the Coulomb repulsion in $BaFe_2As_2$. Figure 1(a) and 1(b) show the frequency dependence of the Slater integrals for Fe-3d orbitals on imaginary frequency axis in linear and log scale, respectively. At very high frequency, the interaction is unscreened and approaches its atomic value. The density-density Coulomb interaction F_0 is strongly screened in the solid, while the higher multipoles F_2 and F_4 are much less energy dependent, and almost equal in solid as in the atom.

The static Coulomb interaction F_0 is estimated to be no less then 5 eV, larger then previously estimated by constrained LDA[11] and constrained RPA.[10] We want to remark that the self-consistency of GW is important in this material, because the non-self consistent version of GW leads to weaker interaction strength $F_0\approx3.4$ eV.

The higher order multipoles F_2 and F_4 show only a weak frequency dependence. The highest multipole F_4 is less screened then F_2, and hence a single number J does not parameterize the form of the Hund's coupling very well, as $J(F_2)\neq J(F_4)$ in Fig. 1(c). Finally Fig. 1(d) shows that the Slater parametrization of the GW Coulomb interaction is remarkably accurate in $BaFe_2As_2$, with error less then 6%.

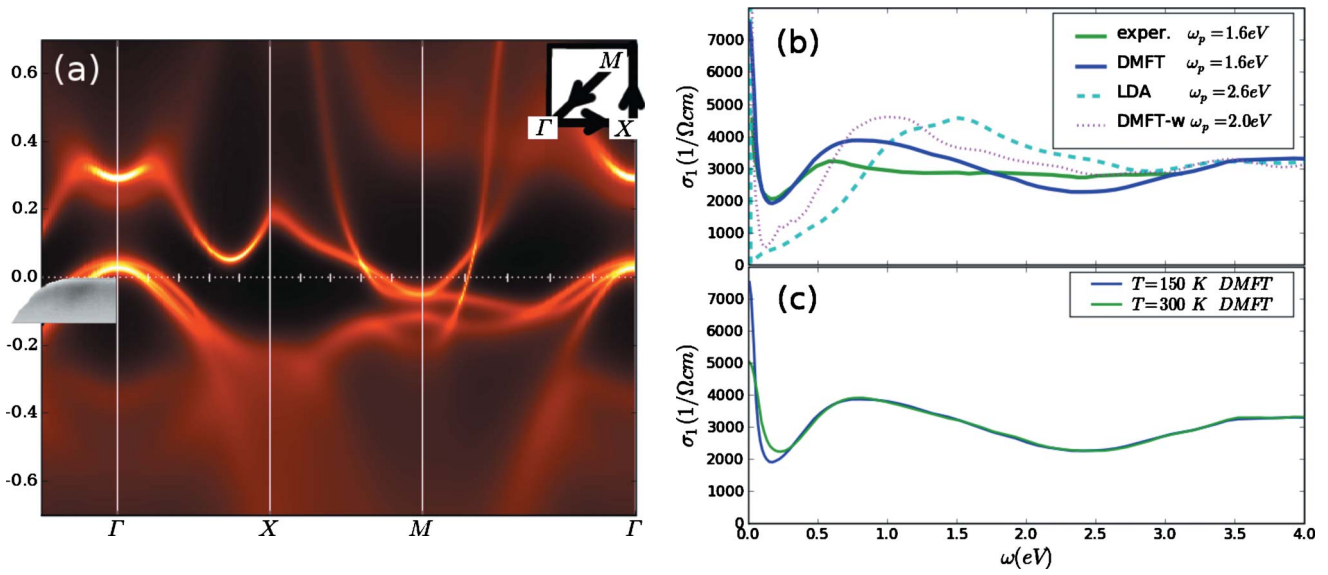

FIG. 2. (Color online) (a) $A(\mathbf{k},\omega)$ of $BaFe_2As_2$ at $T=150$ K as computed by LDA+DMFT. The inset shows the path in momentum space, while the gray inset shows the ARPES intensity from Ref. 9. (b) Optical conductivity of LDA+DMFT method (DMFT) and its comparison with experiment of Ref. 4 (exper.). Also shown is the LDA optical conductivity and LDA+DMFT conductivity with substantially smaller F_0 of Ref. 10 (DMFT-w). The legend contains the strength of the Drude peak, which is broadened only due to electron-electron interactions. (c) Temperature dependence of the optical conductivity within LDA+DMFT.

We now turn to the spectral properties of the $BaFe_2As_2$. Earlier five-band model LDA+DMFT calculations[15] not only displayed important mass renormalization at low energies ($m^*/m \approx 3-5$), but also showed a sharp lower Hubbard band. We now perform computations by newly implemented charge self-consistent LDA+DMFT(CTQMC) method, based on WIEN2K,[29] and explained in detail in Ref. 27. The *GW* estimate for the Slater integrals, renormalized by $1/(1+\alpha)^2=0.91$ due to elimination of the hybridization with semicore states, are $F_0=4.9$ eV, $F_2=6.4$ eV, and $F_4=4.3$ eV. We use the standard localized limit double-counting, which gives for the valence $n_d=6.2\pm0.05$, in perfect agreement with *GW* estimate $n_d=6.2$, hence there is no uncertainty in appropriateness of the chosen double-counting correction. The quasiparticle mass renormalization obtained by DMFT is $Z\sim 1/2$ for lighter x^2-y^2 and z^2 orbitals and $Z\sim 1/3$ for heavier xz, yz and zx orbitals.

In Fig. 2(a), we plot the spectral function $A(\mathbf{k},\omega)$ along the path shown in the inset. There are three circular hole pockets at Γ and two electron pockets at M, in agreement with ARPES[30,31] and LDA. The two smaller pockets are degenerate and their crossing occurs at $0.166\pi/a$ and $0.28\pi/a$, in good agreement with ARPES,[9] where the pocket size was estimated to $0.14\pi/a$ and $0.28\pi/a$, respectively. The Fermi velocities at Γ point toward X, predicted by our method, are ~0.45 eV Å, more then twice smaller then in LDA. The velocity is in reasonable agreement with experiment where somewhat different velocities for the two pockets are estimated to be 0.43 eV Å and 0.32 eV Å.[9] We also overlay the ARPES intensity from Ref. 9 on our spectral dispersion to emphasize good agreement.

The optical conductivity is also a strong test of the correlation strength, as pointed out in Ref. 2. The strong reduction of Drude weight and the presence of midinfrared peak at ~0.6 eV was noticed in Refs. 3 and 4. In Fig. 2(b), we show optics obtained by LDA and by DMFT, and we compare it to experimental results of Refs. 4. Although LDA gives a reasonable order of magnitude for optics, it clearly disagrees with experiments in strength of the Drude peak ($\omega_p \approx 2.6$ eV) and position of the mid-infrared peak, coming from the interband transitions. In contrary our DMFT results give smaller Drude peak of strength $\omega_p=1.6$ eV, in very favorable agreement with experiments.[3,4] We also notice similar width of the Drude peak in DMFT and experiments, which shows that the most important channel for scattering in this material is the electron-electron scattering. Finally, the position of the midinfrared peak, which LDA predicts at frequency ~1.2 eV, appears around 0.6 eV in DMFT, in very favorable agreement with experiment.[3,4]

To demonstrate the sensitivity of the optical conductivity to the strength of the correlations, we carried out LDA+DMFT calculation using parameters of Ref. 10, $F_0=2.69$ eV, $J=0.79$ eV, and $n_d=6.53$. The resulting quasiparticle renormalization amplitude is $Z\sim 0.6$, in very good agreement with results of Ref. 10. In Fig. 2(b) we show optical conductivity thus obtained with label DMFT-w. We noticed that neither Drude peak weight ($\omega_p=2.0$ eV) nor the position of the midinfrared peak (≈ 1 eV) is in good agreement with experiments, thus confirming that $BaFe_2As_2$ should not be regarded as weakly correlated material.

Finally, Fig. 2(c) shows the temperature dependence of optical conductivity as obtained by DMFT. While the interband transitions are roughly temperature independent, the Drude peak width and strength is temperature dependent, substantially sharpening at 150 K compared to 300 K, which is the consequence of the coherence incoherence crossover in this temperature range, discussed in Ref. 32.

Figure 3(a) show the total density of states (DOS) and Fe-3*d* partial DOS. Panel (b) shows the As-4*p* partial DOS.

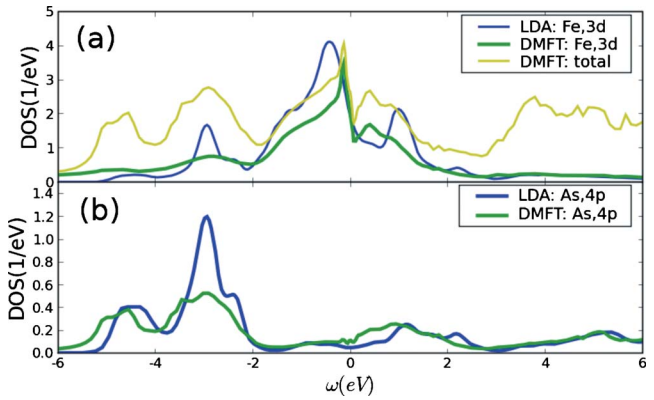

FIG. 3. (Color online) Total and partial density of states of LDA+DMFT method compared to LDA density of states.

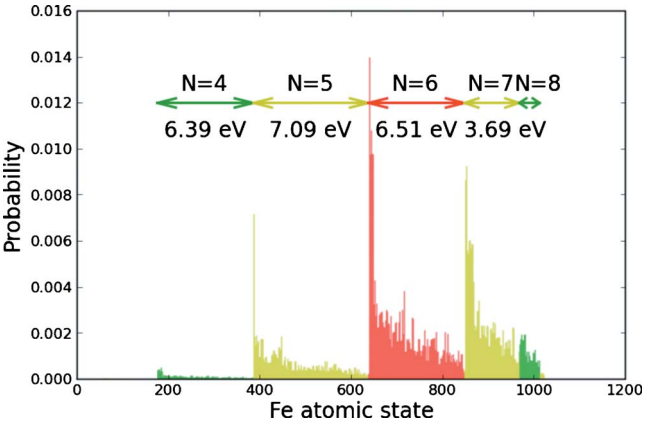

FIG. 4. (Color online) The atomic histogram of the Fe-3*d* shell for $BaFe_2As_2$. The atomic states (all 1024) are sorted according to their valence *N*. Below the arrow we also display the multiplet splitting of the atomic states in each valence. The $N=5$ and $N=6$ valences show the largest splitting of 7 and 6.5 eV, resulting in a very broad lower Hubbard band of the one electron density of states.

Comparing LDA+DMFT partial DOS to LDA partial DOS, we notice that apart from the renormalization of the low energy quasiparticles, and broadening of the high-energy features, there is only little difference between LDA and LDA +DMFT momentum averaged spectral functions. This is in agreement with x-ray absorption spectroscopy,[6] where good agreement between LDA and the experiments was pointed out. Given the strong correlation effects present in optics and low energy ARPES, it is unusual that no clear Hubbard-like satellites of the atomic like $3d^5$ state can be identified in local density of states.

The DMFT valence histogram,[33] describing the probability of finding each Fe-3*d* atomic configuration in the solid as a function of the renormalized energy of the atomic state sheds light on the unusual metallic state of the iron pnictides. In a weakly correlated metal, almost all the atomic configurations are significantly present in the ground state of the solid and their energy vary over the scale of the hybridization which represents the bandwidth of the metal. In correlated oxides, on the other hand, only a few atomic states in each valence have substantial weight, which results in sharp Hubbard bands. As shown in Fig. 4, in $BaFe_2As_2$, the probability of the atomic ground state with valence $N=6$, $N=7$, and $N=5$ is only 0.014, 0.01, and 0.007, respectively. Other states have smaller probability, but remarkably *all* atomic states with valence 5, 6, and 7 have finite probability larger then 0.0005. The large occupancy of the extremely large number of atomic configurations is reminiscent of an itinerant system. On the other hand, unlike the weakly correlated situation, the spread of the multiplets of the $N=5$ states, (coming from the Slater integrals F_2 and F_4) is ~ 7 eV similarly the atomic states with $N=6$ span an energy range of 6.5 eV. This scale, represents the width of the Hubbard bands and is very large, much larger than the scale of the hybridization (2. eV).

We stress that the absence of clear atomiclike satellite excitations is not due to weak correlations in FeAs materials, as suggested in Refs. 10–12, but rather due to the strength of the atomic multiplet splittings and due to the broad bandwidth of the highly polarizable As states. This situation, arises for the parameters determined from the self consistent *GW* method. It is significantly different from what is found in the oxides, and is captured by the charge self-consistent LDA+DMFT calculation.

IV. CONCLUSION

In conclusion, we introduced a self-consistent approach to compute the Coulomb interaction which is tailored to be used with the all-electron DMFT method. It successfully explains the normal state properties of $BaFe_2As_2$, and elucidates the unique nature of the correlations in this material.

ACKNOWLEDGMENTS

We are grateful to Nick Zein, A. Georges, and A. Aichorn for discussion. K.H. was supported by NSF Grant No. DMR-0746395 and Alfred P. Sloan foundation. G.K. and A.K. were supported by NSF under Grant No. DMR-0906943. K.H. and G.K. acknowledge support of NSF under Grant No. DMR 0806937. S.S. was supported by DOE SciDAC (Grant No. SE-FC02-06ER25793). This research was supported in part by the NSF through TeraGrid resources under Grant No. DMR100048, and Blue Waters Grant No. 0941181. The authors also acknowledge KITP for support.

[1] L. Hedin, Phys. Rev. **139**, A796 (1965).
[2] M. M. Qazilbash, J. J. Hamlin, R. E. Baumbach, Lijun Zhang, D. J. Singh, M. B. Maple, and D. N. Basov, Nat. Phys. **5**, 647 (2009).
[3] Z. G. Chen, R. H. Yuan, T. Dong, and N. L. Wang, Phys. Rev. B **81**, 100502(R) (2010).
[4] W. Z. Hu, J. Dong, G. Li, Z. Li, P. Zheng, G. F. Chen, J. L. Luo, and N. L. Wang, Phys. Rev. Lett. **101**, 257005 (2008).
[5] W. L. Yang, A. P. Sorini, C.-C. Chen, B. Moritz, W.-S. Lee, F. Vernay, P. Olalde-Velasco, J. D. Denlinger, B. Delley, J.-H. Chu, J. G. Analytis, I. R. Fisher, Z. A. Ren, J. Yang, W. Lu, Z. X. Zhao, J. van den Brink, Z. Hussain, Z.-X. Shen, and T. P. Devereaux, Phys. Rev. B **80**, 014508 (2009).
[6] C. Parks Cheney, F. Bondino, T. A. Callcott, P. Vllmercati, D. Ederer, E. Magnano, M. Malvestuto, F. Parmigiani, A. S. Sefat, M. A. McGuire, R. Jin, B. C. Sales, D. Mandrus, D. J. Singh, J. W. Freeland, and N. Mannella, Phys. Rev. B **81**, 104518 (2010).
[7] Takeshi Kondo, R. M. Fernandes, R. Khasanov, Chang Liu, A. D. Palczewski, Ni Ni, M. Shi, A. Bostwick, E. Rotenberg, J. Schmalian, S. L. Budko, P. C. Canfield, and A. Kaminski, Phys. Rev. B **81**, 060507(R) (2010).
[8] C. Liu, G. D. Samolyuk, Y. Lee, N. Ni, T. Kondo, A. F. Santander-Syro, S. L. Budko, J. L. McChesney, E. Rotenberg, T. Valla, A. V. Fedorov, P. C. Canfield, B. N. Harmon, and A. Kaminski, Phys. Rev. Lett. **101**, 177005 (2008).
[9] V. Brouet, F. Rullier-Albenque, M. Marsi, B. Mansart, J. Faure, L. Perfetti, A. Taleb-Ibrahimi, P. Le Fevre, F. Bertran, A. Forget, and D. Colson, arXiv:1002.4952 (unpublished).
[10] M. Aichhorn, L. Pourovskii, V. Vildosola, M. Ferrero, O. Parcollet, T. Miyake, A. Georges, and S. Biermann, Phys. Rev. B **80**, 085101 (2009).
[11] V. I. Anisimov, D. M. Korotin, M. A. Korotin, A. V. Kozhevnikov, J. Kunes, A. O. Shorikov, S. L. Skornyakov, and S. V. Streltsov, J. Phys.: Condens. Matter **21**, 075602 (2009).
[12] S. L. Skornyakov, A. V. Efremov, N. A. Skorikov, M. A. Korotin, Yu. A. Izyumov, V. I. Anisimov, A. V. Kozhevnikov, and D. Vollhardt, Phys. Rev. B **80**, 092501 (2009).
[13] I. I. Mazin, arXiv:0910.4117 (unpublished).
[14] D. J. Singh, Physica C **469**, 418 (2009).
[15] K. Haule, J. H. Shim, and G. Kotliar, Phys. Rev. Lett. **100**, 226402 (2008).
[16] Q. Si, E. Abrahams, J. Dai, and J.-X. Zhu, New J. Phys. **11**, 045001 (2009).
[17] L. Craco, M. S. Laad, S. Leoni, and H. Rosner, Phys. Rev. B **78**, 134511 (2008).
[18] H. Ishida and A. Liebsch, Phys. Rev. B **81**, 054513 (2010).
[19] B. Holm and U. von Barth, Phys. Rev. B **57**, 2108 (1998).
[20] A. Kutepov, S. Y. Savrasov, and G. Kotliar, Phys. Rev. B **80**, 041103(R) (2009).
[21] C. O. Almbladh, U. Von Barth, and R. Van Leeuwen, Int. J. Mod. Phys. B **13**, 535 (1999).
[22] Q. Si and J. L. Smith, Phys. Rev. Lett. **77**, 3391 (1996).
[23] R. Chitra and G. Kotliar, Phys. Rev. Lett. **84**, 3678 (2000).
[24] F. Aryasetiawan, M. Imada, A. Georges, G. Kotliar, S. Biermann, and A. I. Lichtenstein, Phys. Rev. B **70**, 195104 (2004).
[25] T. Miyake, F. Aryasetiawan, and M. Imada, Phys. Rev. B **80**, 155134 (2009).
[26] G. Kotliar, S. Y. Savrasov, K. Haule, V. S. Oudovenko, O. Parcollet, and C. A. Marianetti, Rev. Mod. Phys. **78**, 865 (2006).
[27] K. Haule, C.-H. Yee, and K. Kim, Phys. Rev. B **81**, 195107 (2010).
[28] J. Kuneš, I. Leonov, M. Kollar, K. Byczuk, V. I. Anisimov, and D. Vollhardt, Eur. Phys. J. Spec. Top. **180**, 5 (2009).
[29] P. Blaha, K. Schwarz, G. K. H. Madsen, K. Kvasnicka, and J. Luitz, *Wien2K*, edited by Karlheinz Schwarz (Technische Universitat Wien, Austria, 2001).
[30] P. Richard, T. Sato, K. Nakayama, S. Souma, T. Takahashi, Y.-M. Xu, G. F. Chen, J. L. Luo, N. L. Wang, and H. Ding, Phys. Rev. Lett. **102**, 047003 (2009).
[31] P. Richard, K. Nakayama, T. Sato, M. Neupane, Y.-M. Xu, J. H. Bowen, G. F. Chen, J. L. Luo, N. L. Wang, X. Dai, Z. Fang, H. Ding, and T. Takahashi, Phys. Rev. Lett. **104**, 137001 (2010).
[32] K. Haule and G. Kotliar, New J. Phys. **11**, 025021 (2009).
[33] J. H. Shim, K. Haule, and G. Kotliar, Nature (London) **446**, 513 (2007).